Int J Appl Earth Obs Geoinformation 86 (2020) 102011

Contents lists available at ScienceDirect

Int J Appl Earth Obs Geoinformation

journal homepage: www.elsevier.com/locate/jag

Errors related to the automatized satellite-based change detection of boreal forests in Finland

Timo P. Pitkänen[a,*], Laura Sirro[b], Lauri Häme[c], Tuomas Häme[b], Markus Törmä[d], Annika Kangas[e]

[a] Natural Resources Institute Finland (Luke), Latokartanonkaari 9, FI-00790 Helsinki, Finland
[b] VTT Technical Research Centre of Finland Ltd., P.O. Box 1000, FI-02044 VTT, Finland
[c] Terramonitor, Ilmalankatu 2A, FI-00240 Helsinki, Finland
[d] Finnish Environment Institute, Latokartanonkaari 11, FI-00790 Helsinki, Finland
[e] Natural Resources Institute Finland (Luke), Yliopistokatu 6, FI-80100 Joensuu, Finland

ARTICLE INFO

Keywords:
Change monitoring
Forest management
Accuracy assessment

ABSTRACT

The majority of the boreal forests in Finland are regularly thinned or clear-cut, and these actions are regulated by the Forest Act. To generate a near-real time tool for monitoring management actions, an automatic change detection modelling chain was developed using Sentinel-2 satellite images. In this paper, we focus mainly on the error evaluation of this automatized workflow to understand and mitigate incorrect change detections. Validation material related to clear-cut, thinned and unchanged areas was collected by visual evaluation of VHR images, which provided a feasible and relatively accurate way of evaluating forest characteristics without a need for prohibitively expensive fieldwork. This validation data was then compared to model predictions classified in similar change categories. The results indicate that clear-cuts can be distinguished very reliably, but thinned stands exhibit more variation. For thinned stands, coverage of broadleaved trees and detections from certain single dates were found to correlate with the success of the modelling results. In our understanding, this relates mainly to image quality regarding haziness and translucent clouds. However, if the growing season is short and cloudiness frequent, there is a clear trade-off between the availability of good-quality images and their preferred annual span. Gaining optimal results therefore depends both on the targeted change types, and the requirements of the mapping frequency.

1. Introduction

Natural forest dynamics in the boreal zone are characterised by slow growth and occasional disturbances from fire, snow, storms or insect outbreaks, which vary greatly in terms of their severity and extent (Kuuluvainen and Aakala, 2011). Currently, however, about two-thirds of all boreal forests are under some form of management activity, which has largely homogenized the forest structure and suppressed the effects of previous disturbance dynamics (Larsson and Danell, 2001; Gauthier et al., 2015). This is also the case in Finland, where intentional management is the most important factor controlling the structure and function of the boreal forest ecosystem, including tree species distribution, biodiversity, and related ecosystem services (Esseen et al., 1997; Kuuluvainen, 2009). There is some variation between years, but approximately 3.4 % of the total forest land area is annually under management action, of which about 0.9 % are clear-cuts or aim at natural regeneration with deliberately left retention trees, and 2.5 % are related to thinnings, including the removal of seed trees or shelterwood trees (Luke, 2018).

Given the present mechanised and efficient forest industry in Finland and its high economic value, the sustainable management of forest resources with successful biodiversity protection requires careful planning (Kangas et al., 2015; Buongiorno and Gilless, 2003; Bettinger et al., 2017). While sustainability and forest regeneration after clear-cutting are targeted in the Forest Act, monitoring its implementation has been deficient in Finland and has lacked capability to detect forest cuttings independent of the forest owners' own announcements. This resembles the earlier situation in Sweden, where extensive application of satellite imagery for detecting clear-cut areas started in the late 1990s through the Enforma project. After analysing the first set of results, it was found that nearly 10 % of the clear-cut areas per annum differed from the delineations declared by the forest owners, consisting mostly of border deviations of the actually cut area. As evaluated again, by 2003, the proportion of such deviations had dropped to less than 0.5

* Corresponding author.
E-mail addresses: timo.p.pitkanen@luke.fi (T.P. Pitkänen), laura.sirro@vtt.fi (L. Sirro), lauri.hame@terramonitor.com (L. Häme), tuomas.hame@vtt.fi (T. Häme), markus.torma@ymparisto.fi (M. Törmä), annika.kangas@luke.fi (A. Kangas).

https://doi.org/10.1016/j.jag.2019.102011
Received 20 August 2019; Received in revised form 1 November 2019; Accepted 3 November 2019
Available online 04 December 2019

%. The remaining differences were due to unintentional errors instead of deliberate actions (Sawyer et al., 2016).

To monitor and control management activities and support sustainable forest use at the operational level, reliable and up-to-date spatial information on forests is evidently needed. Given that boreal forested areas are large and mostly remote, satellite-based mapping has often been regarded as the most feasible option for collecting relatively accurate information at different scales (Boyd and Dansons, 2005; Hansen et al., 2013; White et al., 2016; Saarinen et al., 2018). However, in Finland, located at high latitudes with relatively low sun angle, short growing season, and often cloudy weather, availability of applicable remote sensing data is limited. These factors by no means prohibit the use of remote sensing for forest mapping purposes, but they increase the pressure to use images of suboptimal quality.

In general, satellite-based change detection applications are usually based on either observing variations over a longer time series or on comparing pixel values between specific dates. Approaches relying on time series, such as BFAST or CCDC, aim to recognize deviations from spectral trends and seasonality, and are best suited to relatively distinct changes using frequent image acquisitions (Verbesselt et al., 2010; Zhu and Woodcock, 2014). Compared to this, a comparison of pixel values recorded between two dates has fewer requirements for data frequency, but its apparent ease is often hindered by e.g. atmospheric or phenological factors, difficulties in image calibration, or otherwise variable image quality (Fuller et al., 2003; Coppin et al., 2004). Strategies to cope with these factors in the analysis phase include approaches to correct their effects, the exclusion of inferior source materials, and the application of methods capable of suppressing their influence. Instead of detecting changes pixel by pixel, a comparison of larger continuous segments, or objects, has recently received increased attention (Chen et al., 2012; Cheng and Han, 2016). Object based analysis can reduce the noise and enable spatial linkages between the adjacent values, but variations in image quality, contemporary reflection characteristics, and acquisition conditions may produce highly variable results, even under stable land cover and perfect co-registration (Hussain et al., 2013; Tewkesbury et al., 2015). In recurrent and operational applications, however, the potential to confirm the quality of single images or change detection results is limited, and quality control must therefore be based on generalised image selection rules and the sufficient robustness of the applied methodology.

Understanding the expected accuracy and potential limitations of the source data is of primary importance in operational forest monitoring, especially if the processing chain is automatized with limited user intervention. Constructing a contingency matrix which indicates errors of inclusion (commission) and exclusion (omission) can be used as a good starting point for statistical evaluation (Lunetta et al., 1991), but validation data specifying the actually occurring changes is needed first. This data can generally be collected by ground measurements or using finer-grained earth observation data compared to the sensor of interest, such as high-resolution satellite images or aerial photos (Kennedy et al., 2009; Xie et al., 2008). Sources of reference data need to be independent of the input material and coincide with the studied change interval, although finding, accessing or processing them is not always straightforward (Cohen et al., 2010; Verbersselt et al., 2010). In addition, particularly when mapping rare events, the inclusion of a sufficient number of focused changes needs to be confirmed. This can be assured by stratifying the region of interest with respect to the expected change characteristics, and collecting an adequate number of samples from each stratum. As a result, the precision of user's accuracy will be improved while simultaneously, estimation of producer's and overall accuracies deteriorate, but this compromise may be needed because of limited accuracy assessment resources (Olofsson et al., 2014).

The balance between commission and omission errors can usually be adjusted by the detection thresholds of the used algorithm, but optimisation and trade-offs between the two greatly depend on the application (Bastarrika et al., 2011; Fraser et al., 2003; Husak et al., 2008). In the context of operational change detection, the minimisation of false positive classifications should principally be emphasised, given that positive predictions are usually the ones requiring further actions. However, not all the changes can be observed at a similar accuracy, which also affects methodological decisions, depending on the intended prioritisation. Fuller et al. (2003) divide changes into "revolutionary", which are distinctive and can be mapped relatively easily, and "evolutionary", which are characterised by a less intensive appearance, fuzzier borders, and a higher level of uncertainty. From the forest management perspective, clear-cut areas should be regarded as revolutionary changes, resulting in obvious and long-term or permanent changes to the existing land cover. Selective logging and other disturbances, which may result in forest degradation but not loss per se, should instead fall into the evolutionary class (Bullock et al., 2018; Hirschmugl et al., 2014; Matricardi et al., 2010). While it should be important to map both in terms of collecting change-related information, clear-cut detections should however be emphasised for sustainable management and a more drastically altered ecosystem structure.

In this paper, we evaluate the sources, effects, and consequences of errors related to automatized detection of management-based forest changes in Finland. The described processing chain was designed for the operational use of the Finnish Forest Centre to monitor intended management actions and to indicate changes without pre-existing information or applicable permits, as stated in the Forest Act. The approach of this study relies on satellite-based change detection, utilising Sentinel-2 images. Validation and accuracy assessment are performed using visually interpreted very high resolution (VHR) satellite images close to the applied Sentinel-2 dates. We especially aim to discern first, the accuracy of the automatically generated change detection results; second, the principal reasons affecting the observed accuracy; and third, how the value and applicability of this approach should be seen from the operational perspective, and potentially differing user needs.

2. Materials and methods

2.1. Study area

The study was performed using five subareas in the boreal zone of Southern and Central Finland (Fig. 1). Each subarea covered 100-137 km^2 having total area of 596 km^2 with the forest proportions ranging between 75.0 and 86.6 %. In terms of tree species, Ähtäri and Virrat were dominated by Scots pine (*Pinus sylvestris*) and Norway spruce (*Picea abies*), whereas the three other areas have a higher proportion of mixed forests, including at least 25 % of broadleaved trees, which are principally silver birch (*Betula pendula*) and downy birch (*Betula pubescens*).

2.2. Change detection modelling

The AutoChange (AC) method, initially presented by Häme et al., 1998 and applied in this study for change detection, is based on a hierarchical unsupervised spectral clustering of bitemporal satellite data. Observations, i.e. spectrally homogeneous groups of pixels, are selected from satellite images, and classified in primary and secondary classes, based on the average reflectance values of observations in the earlier and later images respectively. The change type and magnitude are computed for each image pixel using the spectral properties of the primary and secondary classes to which they belong. Finally, the pixels of the mapped area are labelled to change classes, using the change type, change magnitude and the primary class representing the initial land cover type. To improve the reliability of the AC algorithm, change detection in this study was simultaneously carried out using a set of multi-temporal pairwise comparisons over the whole study period (Fig. 2). The rationale for this was to identify changes which exceed a certain magnitude and can be verified from several image pairs across

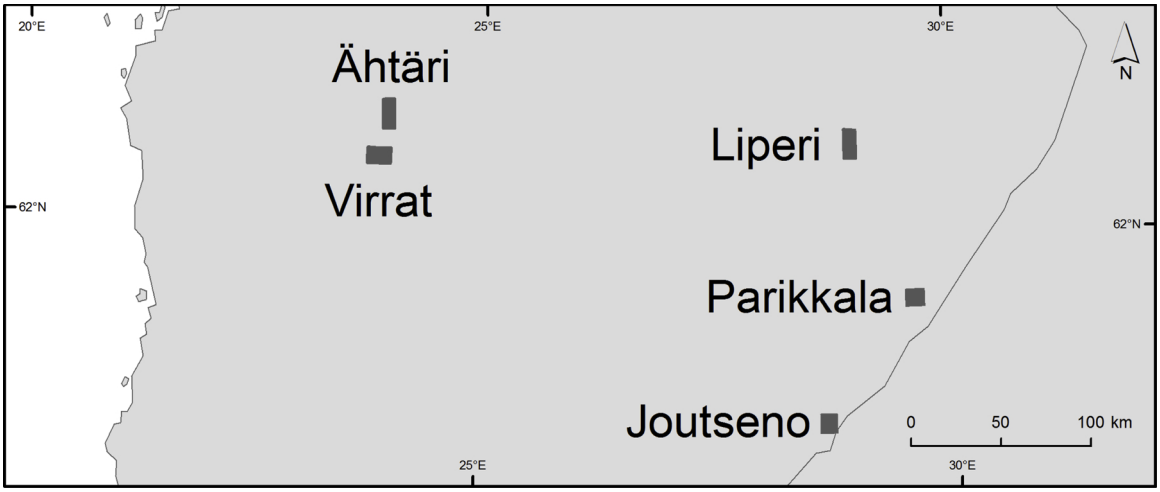

Fig. 1. Map of the study area, indicating five different subareas and their indicative reference names. Background map: © EuroGeographics for the administrative boundaries.

the actual change, thereby suppressing the effects of differences from e.g. atmospheric conditions, weather, or phenology.

Sentinel-2 images from 2015 to 2017, acquired mainly in cloud-free conditions between July and September, were used as a source material for AC modelling. This resulted in the availability of 5–14 suitable images depending on the subarea. As the suitable change magnitude levels for detecting management-related forest changes were unknown, four different pairs of values were tested as cut-off thresholds separating unchanged, thinned, and clear-cut stands. They were initially based on visual evaluation and expected to cover the range of potential values associated with changed areas. Here, these four cases are called sensitivity levels, and named as low, medium-low, medium-high, and high, according to the applied minimum magnitudes to separate the different change types. Further, after detecting the changes at each sensitivity level, the raster-based results were polygonised to create larger consistent areas and remove the effects of single pixels. The minimum mapping unit related for polygonisation was set to 0.5 ha, thus removing smaller areas and interpreting them as unchanged.

2.3. Error evaluation

2.3.1. Data preparation and sampling

Validation data for the AC results was collected by visual interpretation using a set of VHR images. The VHR material consisted of orthorectified multispectral WorldView-2 and Pléiades-1A/B images, both of which had a 0.5 m pan-sharpened resolution (source: CNES 2015-17 distribution Airbus DS; ESA Category-1 projects C1F.33532 and C1F.35754). These VHR images were taken in August or September between 2015 and 2017, thus aiming to minimise seasonal variation and temporally lying within the Sentinel-covered span. From the Ähtäri and Liperi subareas, VHR images were available from years 2015, 2016 and 2017, and from the remaining three subareas from years 2015 and 2016, respectively. Some of the VHR images had a small number of scattered clouds, which were excluded from the validation area.

Changes for error evaluation were interpreted using sample plots, because a manual delineation of changes from the whole study area would have been almost impossible due to limited resources. A single plot was defined as a rectangular 30 m × 30 m area, corresponding to a group of 3 × 3 adjacent Sentinel pixels. This size was regarded as the best compromise, because it was relatively small, but enabled reliable visual interpretation in practice, and was not too strongly influenced by single-pixel errors when applied to validate the AC-based results (Häme et al., 2013).

Plot locations were selected using a stratified random approach to ensure sufficient inclusion of changes. Stratification was based on notifications of forest use, corresponding to the VHR span, which forest owners are obliged to provide to the Finnish Forest Centre concerning planned forest management activities. Three strata were defined: expected clear-cuts, expected thinnings, i.e. stands affected by partial cutting, and expected unchanged areas, which consisted of all the forested land outside of notification areas. However, these notifications allow but do not oblige the specified actions, and have a validity period of three years. This stratification was therefore considered to increase the inclusion of rarer classes (i.e. changes occurring between the two VHR dates) without resulting in an equal allocation between the classes, as recommended by Olofsson et al. (2014).

From each subarea and one-year VHR image span (either only 2015/16, or both 2015/16 and 2016/17), at least 100 randomly located plots per stratum were then selected, using a 75 m minimum spacing between them. The applied minimum distance was intended to prevent overlapping interpretations and reduce the effects of spatial autocorrelation. This resulted in the final number of 2110 validation plots.

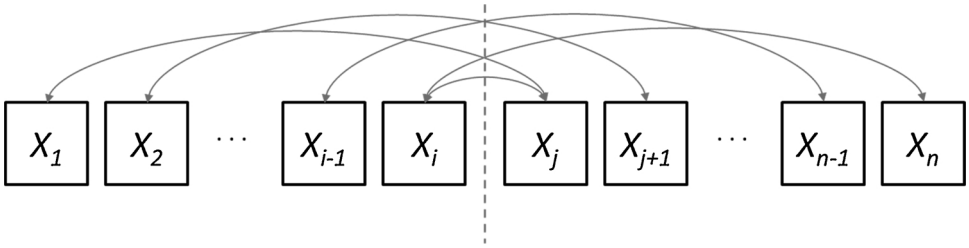

Fig. 2. Multitemporal change detection, applied to a chronological set of satellite images ($X_1 \ldots X_n$). A change (at the dotted line) is expected to be detected in all the pairwise comparisons (arrows), given that image quality is sufficient and the total time interval relatively short, thus allowing confirmed detection of actual changes.

Table 1
Variables interpreted from the sample plots and used in the error evaluation.

Variable	Interpreted From	Explanation
Canopy cover, all	Earlier VHR image	Canopy cover of all trees on forest land (%)
Canopy cover, coniferous trees	Earlier VHR image	Canopy cover of coniferous trees on forest land (%)
Canopy cover, broadleaved trees	Earlier VHR image	Canopy cover of broadleaved trees on forest land (%)
No change	Both VHR images	Proportion of unchanged area (%)
Thinning	Both VHR images	Proportion of thinned area (%)
Wood removal of thinning	Both VHR images	Volumetric proportion of wood removed (%)
Clear-cut	Both VHR images	Proportion of clear-cut area (%)
Soil type	External data	Separation to mineral soil and peatland

2.3.2. Visual interpretation of changes

The generated sample plots were visually interpreted in terms of their forest characteristics and related changes. First, it was confirmed that more than half of the plot area actually belonged to forest land both before and after image acquisitions, and that there were no significant obstacles to hinder the interpretation, such as strong cloud shadows. In this context, the concept of forest land refers to areas designated for or having the potential to be used for productive forestry, therefore being independent of the current tree cover. Given that these conditions were fulfilled, a set of variables as presented in Table 1 was interpreted, mainly using the earlier image (background variables), or both images (change-related variables). False-colour images were used in the interpretation, allowing distinguishing between coniferous and deciduous trees. Separation of clear-cuts from thinned stands was based on the remaining canopy cover so that management activities resulting in less than 10 % canopy cover were defined as clear-cuts. Volumetric wood removal due to thinning was mainly estimated by the decreased canopy cover and evaluated in steps of 10 %. Fig. 3 exemplifies the VHR images overlaid with sample squares, which were interpreted as clear-cut and thinned. Soil type, categorising the plot as predominantly mineral soil or peatland, was extracted directly from the multi-source Finnish National Forest (MS-NFI) Inventory data from 2015.

Interpretations were performed by two skilled persons with experience of forest research, including regular communication throughout the process, and confirmed by a third person. However, as field verifications were not included in the process, the accuracy of these expert opinions may be influenced by various factors such as illumination conditions, the degree of the satellite off-nadir position, and forest characteristics as such. Nevertheless, visual interpretation can be regarded as sufficient for indicating the essential relative differences between the plots, and has been used for long in the Nordic countries for forest inventory purposes (Næsset, 2014).

The processed sample plots were labelled as clear-cut, thinned, and unchanged. To be classified as changed in general, at least half the plot area had to be clear-cut or thinned. The final class was defined by the larger proportion of the two, or assigned as clear-cut in case of even proportions. If no changes were registered or less than half the plot had changed, the plot was labelled as unchanged. Clear-cut patches of less than 0.5 ha were not recognised as changed to make the minimum mapping unit comparable to the AC-based results.

2.3.3. Definition of AC classes

AC-modelled changes were used to define AC classes for the sample plots (Fig. 4). This considered both the existence of AC polygons and the shortest pair of dates between which the change had been detected, given that AC modelling included all the available data from the study period, whereas VHR-based validation data was collected using fixed one-year spans only. First, AC-detected change polygons were overlaid by the sample plots (1), and their within-plot areas were calculated (2). If no polygon overlay was found, or potential change covered less than

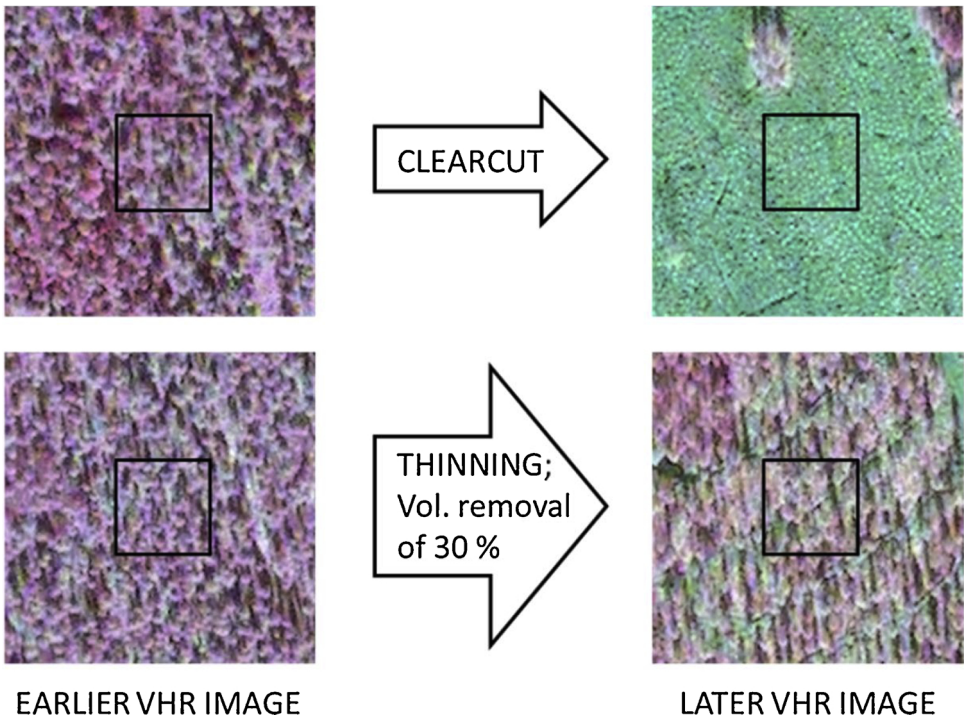

Fig. 3. Examples of clear-cut and thinning detection.

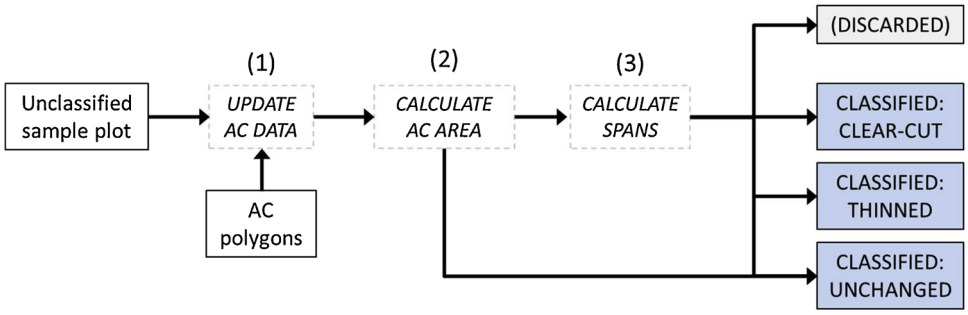

Fig. 4. Process of determining AC classes for unclassified sample plots. The numbers are referred to in the text.

half the plot, the AC class was defined as unchanged.

For the remaining plots, both VHR and AC spans and their coincident span were calculated (3). If there was no coincident span, i.e. dates of the AC-predicted change fell outside the VHR dates, the AC class was defined as unchanged with respect to the VHR validation. If a coincident span was found, and it covered at least half the total AC span (i.e. the modelled change expected to have happened within the VHR span), the AC class was defined as thinned or clear-cut, according to the predicted change or the larger of the two if both existed. If a coincident span was found but covered less than half the total AC span, the sample square was discarded from further analyses. In this case, AC-predicted change was considered to be uncertain with respect to the validation span and therefore not applicable for error evaluation. Discarded plots were not the same at all the sensitivity levels as changes had been predicted separately for each of them, thus having potentially different pairs of Sentinel-2 dates as compared to the validation spans. As a result, the final number of sample plots was between 1944 and 2024 depending on the sensitivity level. Most discarded plots were found at a low sensitivity level, followed by the highest area covered by AC polygons and therefore the greatest chance of span-derived problems.

Furthermore, AC changes covering less than half the sample plot were also observed, and distances to the nearest clear-cut and thinned polygons with a coincident span were calculated from the plot edge. This information was used to mitigate the potential effects of georectification inaccuracies, resolution differences, and polygon-derived generalisations using three additional filtering steps:

1) Plots including more than one VHR-interpreted change classes were removed, resulting in a subset of fully unchanged, thinned, or clear-cut plots regarding the validation data;
2) If a plot was VHR-classified as thinned or clear-cut, and a similar AC polygon overlapped the plot at least marginally (without minimum coverage requirements), the AC class was assigned to correspond with the VHR class; and
3) If a plot was VHR-classified as changed, and a similar and coincident AC polygon was found within 25 m of the plot edge, the AC class was assigned to correspond with the VHR class.

2.3.4. Calculation of errors

Errors were evaluated by error matrices and overall accuracies, as well as further indices described below. Overall accuracies were calculated separately for each stratification layer and added, weighted by their proportional areas, as suggested by Olofsson et al. (2014). The frequently used Cohen's kappa values have been criticised for being inefficient, misleading, or flawed, and were therefore not calculated (Pontius and Millones, 2011; Congalton and Green, 2019; Olofsson et al., 2014). Errors were instead evaluated using precision, recall, and F_1 metrics, which have recently received more attention in remote sensing classification approaches (Liasis and Stavrou, 2016; Matton et al., 2015; Petitjean et al., 2012). They are based on the comparison of true positive (P^T), false positive (P^F), and false negative (N^F) predictions, which generally relate to the Boolean-type existence and non-existence of the observed phenomenon. In the context of this study, two categories were formed by comparing unchanged sample plots to changed ones, i.e. grouping thinning and clear-cut classifications together. Consequently, these three metrics should be regarded as indicating whether changes in general were successfully extracted from unchanged plots, but the applied threshold between thinnings and clear-cuts should be disregarded.

Precision, recall and F_1 are defined as (1)

$$Precision = \frac{P^T}{P^T + P^F};$$
$$Recall = \frac{P^T}{P^T + N^F} \text{ and}$$
$$F_1 = \frac{2 \times Precision \times Recall}{Precision + Recall} \quad (1)$$

Precision indicates the success rate of positive predictions, and recall the ability of the model to capture actual positive instances. F_1, in turn, is a harmonic mean between the precision and recall statistics, therefore providing a single-metric evaluation of the user's and producer's accuracies, similar to kappa. All these metrics were calculated as percentages.

3. Results

3.1. Predicted and observed changes

AC detection results varied substantially, depending on the sensitivity level. Table 2 indicates the number of single change patches (AC polygons), their total area, and the proportion of the total forest area within all five subareas. With the lowest sensitivity, changed areas covered 12.49 % of the total forested area, which is a relatively large proportion compared to the known average coverage of annual forest management actions. In terms of the proportional division between the thinned and clear-cut areas, thinnings were also observed considerably more than at any other sensitivity level. With higher sensitivities, detections of thinned patches dropped more drastically than clear-cuts. At the highest level, the mutual proportions of thinned and clear-cut areas were the opposite of the lowest level, and the detections of changed areas in general dropped to only 2.67 % of the total forest area.

In terms of the VHR-based validation plots, 79.5 % were detected as unchanged, 7.2 % as thinned, and 13.4 % as clear-cut. Regardless of the

Table 2
Results of AC change detections at different sensitivity levels.

Sensitivity	Thinned patches		Clear-cut patches		All changes
	Number	Total area (ha)	Number	Total area (ha)	Proportion of total forest area
Low	1268	4677	908	1436	12,49 %
Medium-low	519	1445	784	1227	5,46 %
Medium-high	257	694	681	1076	3,62 %
High	129	328	624	977	2,67 %

Table 3
Accuracy assessment of AC detections at different sensitivity levels, including statistics related to producer's accuracy (PA), user's accuracy (UA), and metrics described in the text.

a. low sensitivity

	VHR / unch.	VHR / thin.	VHR / cl.-cut	*UA*
AC / unch.	**1428**	**86**	**48**	91.4 %
AC / thin.	**99**	**44**	**4**	29.9 %
AC / cl.-cut	**18**	**7**	**210**	89.4 %
PA	92.4 %	32.1 %	80.2 %	*n=1944*
		Overall accuracy:		**95.4 %**
		Precision:		**69.4 %**
		Recall:		**66.4 %**
		F_1:		**67.9 %**

b. medium-low sensitivity

	VHR / unch.	VHR / thin.	VHR / cl.-cut	*UA*
AC / unch.	**1537**	**109**	**46**	90.8 %
AC / thin.	**31**	**29**	**6**	43.9 %
AC / cl.-cut	**15**	**4**	**210**	91.7 %
PA	97.1 %	20.4 %	80.2 %	*n=1987*
		Overall accuracy:		**98.1 %**
		Precision:		**84.4 %**
		Recall:		**61.6 %**
		F_1:		**71.2 %**

c. medium-high sensitivity

	VHR / unch.	VHR / thin.	VHR / cl.-cut	*UA*
AC / unch.	**1577**	**121**	**57**	89.9 %
AC / thin.	**13**	**23**	**2**	60.5 %
AC / cl.-cut	**12**	**2**	**203**	93.5 %
PA	98.4 %	15.8 %	77.5 %	*n=2010*
		Overall accuracy:		**98.7 %**
		Precision:		**90.2 %**
		Recall:		**56.4 %**
		F_1:		**69.4 %**

d. high sensitivity

	VHR / unch.	VHR / thin.	VHR / cl.-cut	*UA*
AC / unch.	**1601**	**134**	**69**	88.7 %
AC / thin.	**2**	**12**	**0**	85.7 %
AC / cl.-cut	**11**	**2**	**193**	93.7 %
PA	99.2 %	8.1 %	73.7 %	*n=2024*
		Overall accuracy:		**98.9 %**
		Precision:		**94.1 %**
		Recall:		**50.5 %**
		F_1:		**65.7 %**

Table 4
Adjusted plot error statistics of the medium-low sensitivity level (b–d) compared to the initial errors (a).

a. initial accuracy at medium-low sensitivity

	VHR / unch.	VHR / thin.	VHR / cl.-cut	*UA*
AC / unch.	**1537**	**109**	**46**	90.8 %
AC / thin.	**31**	**29**	**6**	43.9 %
AC / cl.-cut	**15**	**4**	**210**	91.7 %
PA	97.1 %	20.4 %	80.2 %	*n=1987*
		Overall accuracy:		**98.1 %**
		Precision:		**84.4 %**
		Recall:		**61.6 %**
		F_1:		**71.2 %**

b. only fully unchanged, thinned or clear-cut plots

	VHR / unch.	VHR / thin.	VHR / cl.-cut	*UA*
AC / unch.	**1494**	**85**	**11**	94.0 %
AC / thin.	**31**	**26**	**3**	43.3 %
AC / cl.-cut	**4**	**2**	**150**	96.2 %
PA	97.7 %	23.0 %	91.5 %	*n=1806*
		Overall accuracy:		**98.4 %**
		Precision:		**83.8 %**
		Recall:		**65.3 %**
		F_1:		**73.4 %**

c. as b, but partial AC changes accepted

	VHR / unch.	VHR / thin.	VHR / cl.-cut	*UA*
AC / unch.	**1494**	**81**	**4**	94.6 %
AC / thin.	**31**	**30**	**1**	48.4 %
AC / cl.-cut	**4**	**2**	**159**	96.4 %
PA	97.7 %	26.5 %	97.0 %	*n=1806*
		Overall accuracy:		**98.4 %**
		Precision:		**84.6 %**
		Recall:		**69.3 %**
		F_1:		**76.2 %**

d. as b, but AC changes within 25 m accepted

	VHR / unch.	VHR / thin.	VHR / cl.-cut	*UA*
AC / unch.	**1494**	**78**	**4**	94.8 %
AC / thin.	**31**	**33**	**1**	50.8 %
AC / cl.-cut	**4**	**2**	**159**	96.4 %
PA	97.7 %	29.2 %	97.0 %	*n=1806*
		Overall accuracy:		**98.4 %**
		Precision:		**84.8 %**
		Recall:		**70.4 %**
		F_1:		**76.9 %**

used stratification scheme, the vast majority of the plots exhibited no observable changes, or the expected management activities had already occurred. According to the external soil type data, 87.0 % of the plots were located on mineral soil and 13.0 % on peatland.

3.2. Errors at different sensitivity levels

Table 3 presents the error matrices and results of the calculated metrics. In all cases, overall accuracies are high, but they are especially driven by the large proportion of unchanged plots. The high sensitivity level reaches the highest overall accuracy, whereas according to the F_1 statistics, medium-low intensity represents the best achievable compromise among the tested sensitivity levels. In general, clear-cut plots are identified quite reliably by AC, whereas thinned areas show more variation.

The medium-low sensitivity, achieving the highest F_1 score, was selected for further adjustment steps as described in Chapter 2.3.3 (Table 4). Compared to the initial non-adjusted errors (a), the removal of plots located at VHR-based transitions (b) decreased the total amount of plots to 1806 and improved both overall accuracy and F_1 score. Further adjustments (c, d) resulted in a further increase of F_1 of up to 76.9 %, but overall accuracy showed only minor changes due to large

Table 5
Problems and their potential causes related to AC-based clear-cut predictions.

Actual clear-cut predicted as unchanged (n = 4)
- Two plots were located within the same clear-cut patch (1.3 ha), which was previously a relatively sparse broadleaved-dominated forest in the vicinity of a farmhouse (Fig. 5a,b)
- One plot was on a small (0.6 ha) new patch extending to a previously clear-cut area along its southern edge, visually suffering from tree shadows (Fig. 5c,d)
- One plot was in a large clear-cut area, part of which was correctly predicted as clear-cut but remaining parts only as thinned or unchanged

Actual clear-cut predicted as thinned (n = 1)
- A plot located on a relatively small clear-cut (1 ha) patch of broadleaved-dominated forest (Fig. 5e,f)

Actual thinning predicted as clear-cut (n = 2)
- One plot was a thinned patch estimated to have 30 % wood removal within the sample plot but higher volumetric change in other parts of the patch (Fig. 5g,h)
- One plot was on a large thinning with 50 % volumetric change, partly predicted as clear-cut

Actual unchanged predicted as clear-cut (n = 4)
- One plot was partly within a small clear-cut area (0.3 ha) which, according to the applied minimum mapping unit, had been classified as unchanged, but predicted by AC to exceed the limit of 0.5 ha.
- Three remaining plots had no obvious reason to be predicted as clear-cut. After a visual check using Sentinel-2 images, however, these were confirmed to have actually been cut after the VHR span but before the later AC date. Therefore, these plots should not be regarded as errors.

proportion of unchanged areas. For reference, the average distance from an unchanged plot to the nearest AC thinning polygon was 496 m, and to the nearest clear-cut polygon 437 m, which indicates that the applied 25 m buffer zone (d) was unlikely to include AC-based changes by chance.

3.3. Observed errors in details

The results corresponding to Table 4 d were applied to estimate the sources of the AC prediction errors in detail, anticipating that they had the best ability to indicate deficiencies related to the actual prediction technique. First, problems of missed or falsely detected clear-cut areas were checked manually, as they were relatively few. These results are presented in Table 5, and a set of related images in Fig. 5. In terms of the subareas, Liperi had most deficiencies (6, including all actual clear-cuts predicted as unchanged and two actual thinnings predicted as clear-cut) whereas the remaining areas showed little variation (Ähtäri 2, Virrat 1, Parikkala 1, and Joutseno 1) (Fig. 5).

Confusion between unchanged and thinned areas was the most common type of error in the classifications. These errors were analysed using the data from visually observed forest characteristics (Table 6). For unchanged plots (a), erroneous predictions (i.e. predicted as thinned) were primarily related to higher canopy cover, and especially broadleaved trees. For thinned plots (b), which had been predicted as unchanged, total canopy coverage did not gain similar importance but wrongly predicted cases were generally characterised by a significantly low coverage of coniferous trees and a high coverage of broadleaved trees. For all plots with thinning-related errors (unchanged, predicted as thinned, or thinned, predicted as unchanged), broadleaved trees had an average canopy coverage of 17 % which exceeded the coverage of coniferous trees on 18 % of plots. On plots predicted correctly as unchanged or thinned, these proportions were 12 % and 9 %, respectively. None of the five subareas stood out in having a particularly high or low number of these confusion errors.

The dates of the Sentinel-2 images that were used in the change detection seemed to affect the success of thinning detections. Most of the Sentinel-2 images were acquired between mid-July and mid-September, but single images appeared to have a particular influence on the results. For thinnings that had been predicted correctly, 42 % were based on the same pair of dates, having an earlier image from 30 August 2015 and later image from 13 September 2016. According to the visual inspection of Sentinel-2 images, both these dates were of good quality and acquired on a clear weather, especially the latter. In unchanged plots which had been predicted as thinned, no similar dominant pair of dates could be recognised. The most obvious anomaly was the Parikkala subarea, with 28.8.2016 used as a later Sentinel-2 date, consisting of almost 20 % of all the wrongly predicted thinnings. This particular image suffered from multiple small cirrus clouds, their shadows, and haziness, which, however, were not considered a sufficient reason to totally reject this image. This was supported by the small number of applicable images available for 2016.

The effect of soil type on change categories was evaluated using Pearson's Chi-squared test, with similar categories to those in Table 6. For unchanged plots, no significant differences were found between mineral soil and peatland but for thinnings, mineral soil was significantly ($p < 0.01$) over-represented in the erroneous predictions. However, this can also be interpreted as emphasising broadleaved trees, given that their canopy cover was generally greated on mineral soil compared to peatland.

4. Discussion

This study confirms the applicability of satellite-based change detection for detecting forest changes from the operational perspective, which requires monitoring of forest changes over a vast area with limited resources, high level of automatization, and predetermined update schedules. This sets a need to use the available satellite images rather than wait for those of better quality, and produce results without considerable bias to any specific forest type. As these factors were satisfied in the presented AC analysis, the Finnish Forest Centre has already implemented the satellite image based change detection as a part of their routines. This releases resources to focus only on those changes which deviate considerably from the submitted forest use notification, or for which no notification has been provided.

The challenge in change detection lies in both achieving and retaining high levels of accuracy to produce reasonably reliable results time after time (Fuller et al., 2003), which must be recognised as prerequisites for operational applications. Furthermore, as this study demonstrates, good overall accuracy will not be a proper measure for detecting relatively rare events: applied thresholds should be determined based on the targeted use. Change detection capabilities are largely determined by whether the applied change magnitude exceeds the signal-to-noise ratio, which can to some extent be improved by applicable pre-processing strategies as well as inclusion of several images instead of an image pair (Kennedy et al., 2010; Verbesselt et al., 2012). Drastic differences such as clear-cuts will generally exceed this threshold, but partial changes like thinning actions may cause complications, due both to their vaguer effects and inconsistent relationships with reflectance values around near-infrared wavelengths (Healey et al., 2006), which may partly explain the errors found in this study.

Forest changes in the boreal zone, including logging activity, windfall damage, and wildfires, have been detected at user's accuracies between 75 and 98 %, depending on the magnitude of the change, study area, applied methodology, and images used in change mapping (Baumann et al., 2014; Hermosilla et al., 2015; Pickell et al., 2014; Potapov et al., 2011; Schroeder et al., 2011). Accuracy in detecting clear-cut areas in this study reaches similar levels, but success in the detection of thinned stands is considerably lower. Measurements of accuracy and classification performance, however, must always be interpreted in the context of the study area and applied change categories. One of the closely corresponding earlier studies is that of Ala-Sisto and Packalen (2016), who interpreted similar forest changes with LiDAR data close to the areas used in our study. They achieved an accuracy of 98.6 % for the detection of clear-cuts but only 24.1 % for thinnings, which resembles the results presented in this paper. It should also be stressed that our accuracy assessment was performed using manually interpreted VHR images, thus potentially indicating minute differences which may not be practically detectable from coarser

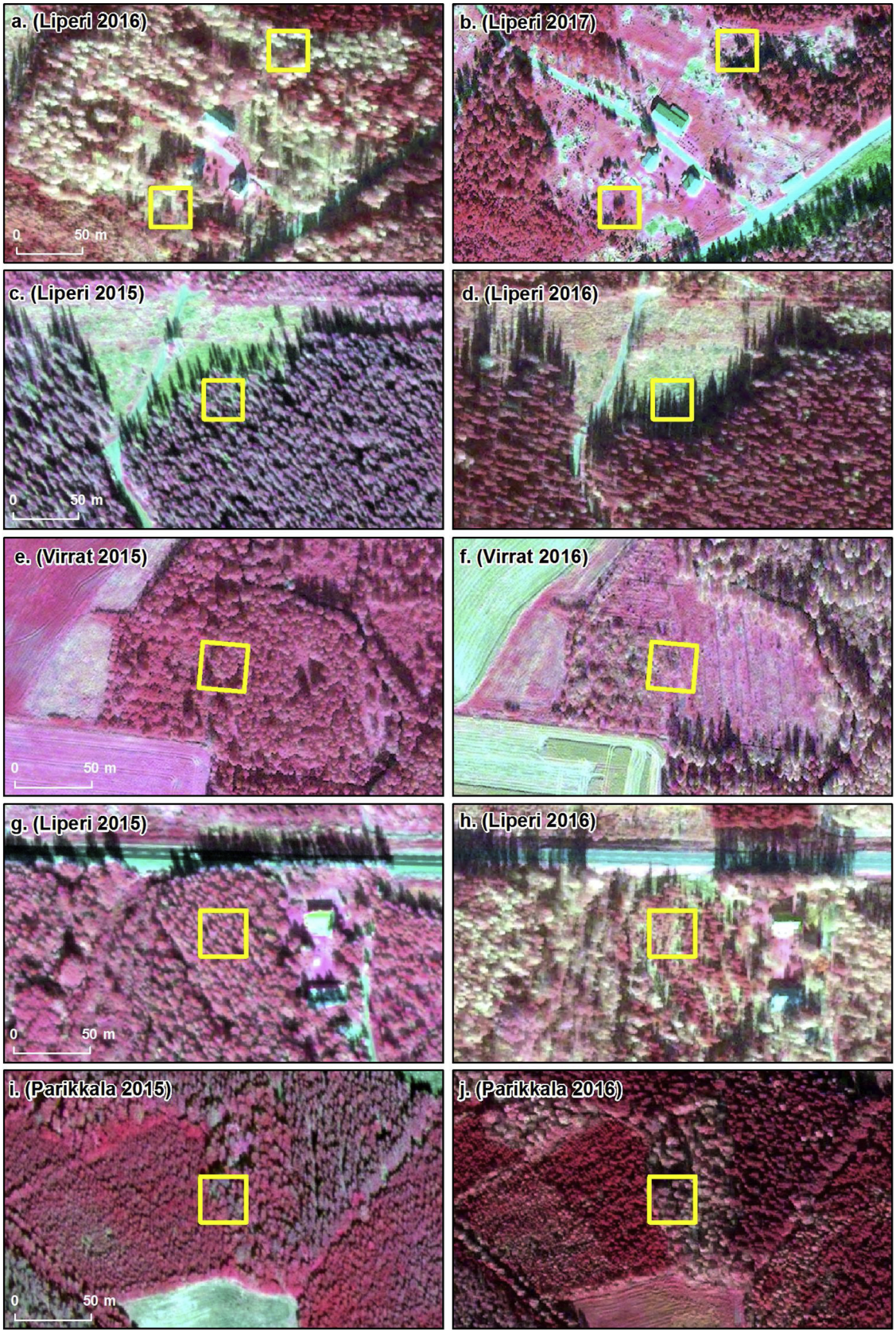

Fig. 5. Examples of clear-cut detection problems on VHR images. Details are explained in Table 5.

resolution images.

Thinning-related errors appear to be affected by a higher proportion of broadleaved trees, which is likely to be related to both structural heterogeneity and higher spectral fluctuation compared to stands dominated by coniferous trees. Broadleaved trees at high latitudes are also characterized by seasonal variation, causing extremities which

Table 6
Significance levels (p values, according to two independent samples t-test) when comparing the successful and unsuccessful predictions of unchanged (a) and thinned (b) plots. Bold font indicates positive errors, with significant ($p < 0.05$) differences coloured in red. Correspondingly, italic font and blue indicate negative errors. Variables presented in the table are the canopy cover of all trees (cc/all), coniferous trees (cc/con), and broadleaved trees (cc/bro), as well as proportional volumetric removal (vol/rem) for thinned plots.

	cc/all	cc/con	cc/bro	vol/rem
a)	**< 0.01**	*0.31*	**0.02**	NA
b)	**0.58**	*< 0.01*	**< 0.01**	**0.90**

a. Unchanged plots, predicted as unchanged vs. predicted as thinned
b. Thinned plots, predicted as thinned vs. predicted as unchanged

from the perspective of remote sensing should be seen primarily as two different types of vegetation (Shao and Wu, 2008; Verbersselt et al., 2010). The transitions between the seasons, especially during autumn, can cause serious complications for change detection due to the fluctuation of satellite-derived reflectance values as a response to the senescence of broadleaved trees (Rautiainen et al., 2012). Our results did not indicate particular deterioration of the results if using relatively late dates, but images applied in the study were taken before the major phenological changes which on this study area are known to normally happen during the latter half of September (Peltoniemi et al., 2018; Poikolainen et al., 2016; Pudas et al., 2008a, b).

Dominance of certain image dates with both correctly and falsely predicted thinnings indicates that image quality is in the key role in successful change detection. As AutoChange method relies on detecting changes between primary and secondary classes rather than comparing reflectance values of single pixels per se, minor atmospheric deviations affecting the whole image frame should not particularly deteriorate the resulting quality. Partially translucent clouds and their shadows in the later image, pose however more complications for the results, even if the change is confirmed using a later image. Translucent clouds absorb near-infrared radiation regardless of their relatively small optical depths, and cloud shadows decrease direct components of the Earth-emitted radiation while having less effects on the reflected radiation (Minnis et al., 1993; Richter and Müller, 2005). These factors, given that AutoChange method does not include spatially linked detection methodology (i.e. connected to the shape of the potentially changed patch), are likely to induce falsely detected biomass losses and consequent thinning predictions.

An obvious improvement to mitigate effects related to image quality would be to select only completely cloudless images, which are sorted out using an objective evaluation strategy. However, this result in a clear trade-off with image availability, given that the growing season in Finland is short, and clouds usually cover 40–60 % of the land area, requiring several satellite passes to construct a cloud-free map (Karlsson, 2003; Sawyer et al., 2016). During our study period, images from 2016 were particularly cloudy and some of the subareas did not have a single totally cloud-free image. Operational targets for change detection require relatively frequent updates, so improving the detection of thinned stands would need methodological updates either increasing the change detection performance, or exclusion of cloud-contaminated parts of the images.

The above considerations and methodological choices applied in this study can be summarised in a few key findings. First, while the AC-based change detection results are themselves quite reliable, verifying the change using several image pairs does not suppress all the noise and variability related to partial forest changes. As satellite images with suboptimal quality may be needed, and a total exclusion of cloud-related effects would result in larger data gaps, a certain number of errors of both omission and commission with the present processing chain are to be expected. Furthermore, these errors are not fundamentally determined by visually observable change intensities but rather relate to spectral characteristics which are difficult to quantify. As AC is based on clustering only in the spectral domain, however, the addition of spatial linkages and neighbourhood relations could assist in this matter, and provide strategies to identify continuous patches of spectral deviations.

Second, to ensure the extraction of actual errors instead of incidental modelling artefacts, the applied evaluation strategy needs to be planned to account for potentialities of both spatial and temporal mismatches. Spatial errors derive from co-registration deficiencies and difficulties in delineating similar features, and temporal errors relate to the differing spans of the modelling and validation materials. In addition, given that extensive fieldwork is often an unfeasible solution for collecting validation data, visual evaluation has potential to offer a workable alternative capable of indicating the principal factors affecting the accuracy.

Third, while one of the several calculated sensitivity levels was given particular attention in our analysis, it should be acknowledged that any of the levels may be the most applicable choice for other purposes, regardless of their apparently higher errors. Different sensitivity levels will offer only a limited number of Boolean-type classifications which have certain drawbacks compared to fuzzy classifications, i.e. having a range of memberships with potential to be divided into distinct classes at any user-defined value (Fisher, 2010). Due to the AC methodology which extracts only changes exceeding certain thresholds using multiple satellite images, however, full fuzziness implementation would be almost impossible or at least require a substantial increase in processing resources. An example of additional uses could be mapping of insect outbreaks, which are challenging to implement reliably at operational level because of their variable spectral signals and intensities (Rullan-Silva et al., 2013; Senf et al., 2017), but could be at least partly detected using the relatively low levels.

Finally, given that one of the primary interests was to test the applicability of this approach from the operational perspective, we analysed if specific forest characteristics influenced the errors and potentially affected the generalisability of the results. While a single evaluation should be primarily seen as a starting point for an iterative improvement process, the errors in our results indicated no critical dependencies on the observed variables except for the proportion of broadleaved trees and deficiencies of the source images. This supports the applicability of the approach for operational use until further adjustments and additional developments are proposed as a result of the search for optimal results and trade-offs.

5. Conclusions

Remote sensing has the capacity to offer powerful tools for automatized change detection, which may provide a comprehensive interpretation of the area of interest and assist in focusing resources on the most applicable targets. However, deficiencies in the image quality appear to impede the results, regardless of whether several image pairs are applied to confirm a change. This especially concerns the detection of thinnings, while the distinguishing of clear-cuts appears not to be affected similarly. However, the applicability of satellite images needs to be evaluated from the perspective of the intended use, which in operational use emphasises greater analysis frequency and the flawless detection of clear-cuts. From this perspective, the results presented in this paper fulfil these requirements with only minor inaccuracies and justify the use of suboptimal images. Further work should be targeted at methodologies interpreting changes at a more comprehensive level, such as advanced machine learning algorithms and deep learning, which might help to incorporate more complex dependencies as well as spatial linkages in the analysis.

Declaration of Competing Interest

We have no conflicts of interest regarding to this manuscript.

Acknowledgements

This work was supported by Ministry of Agriculture and Forestry of Finland through the key project “Wood on the move and new products from forests”.

References

Ala-Sisto, D., Packalen, P., 2016. Forest change detection by using point clouds from dense image matching together with a LiDAR-derived terrain model. IEEE J. Sel. Top. Appl. Earth Obs. Remote Sens. 10, 1197–1206.
Bastarrika, A., Chuvieco, E., Martín, M.P., 2011. Mapping burned areas from Landsat TM/ETM+ data with a two-phase algorithm: balancing omission and commission errors. Remote Sens. Environ. 115, 1003–1012.
Baumann, M., et al., 2014. Landsat remote sensing of forest windfall disturbance. Remote Sens. Environ. 143, 171–179.
Bettinger, P., Boston, K., Siry, J., Grebner, D., 2017. Forest Management and Planning, 2nd ed. Academic Press, Cambridge.
Boyd, D.S., Dansons, F.M., 2005. Satellite remote sensing of forest resources: three decades of research development. Prog. Phys. Geogr. 29, 1–26.
Bullock, E.L., Woodcock, C.E., Olofsson, P., 2018. Monitoring tropical forest degradation using spectral unmixing and Landsat time series analysis. Remote Sens. Environ p. In press.
Buongiorno, J., Gilless, J., 2003. Decision Methods for Forest Resource Management. Academic Press, Cambridge.
Cheng, G., Han, J., 2016. A survey on object detection in optical remote sensing images. ISPRS J. Photogramm. Remote. Sens. 117, 11–28.
Chen, G., Hay, G.J., Carvalho, L.M., Wulder, M.A., 2012. Object-based change detection. Int. J. Remote Sens. 33, 4434–4457.
Cohen, W.B., Yang, Z., Kennedy, R., 2010. Detecting trends in forest disturbance and recovery using yearly Landsat time series: 2. TimeSync — tools for calibration and validation. Remote Sens. Environ. 114, 2911–2924.
Congalton, R.G., Green, K., 2019. Assessing the Accuracy of Remotely Sensed Data: Principles and Practices, 3rd ed. CRC Press, Boca Raton.
Coppin, P., Jonckheere, I., Nackaerts, K., Muys, B., 2004. Digital change detection methods in ecosystem monitoring: a review. Int. J. Remote Sens. 25, 1565–1596.
Esseen, P.-A., Ehnström, B., Ericson, L., Sjöbert, K., 1997. Boreal forests. Ecol. Bull. 46, 16–47.
Fisher, P.F., 2010. Remote sensing of land cover classes as type 2 fuzzy sets. Remote Sens. Environ. 114, 309–321.
Fraser, R.H., Fernandes, R., Latifovic, R., 2003. Multi-temporal mapping of burned forest over Canada using satellite-based change metrics. Geocarto Int. 18, 1–11.
Fuller, R.M., Smith, G.M., Devereux, B.J., 2003. The characterisation and measurement of land cover change through remote sensing: problems in operational applications? Int. J. Appl. Earth Obs. Geoinf. 4, 243–253.
Gauthier, S., et al., 2015. Boreal forest health and global change. Science 349, 819–822.
Hansen, M.C., et al., 2013. High-resolution global maps of 21st-Century forest cover change. Science 342, 850–853.
Healey, S.P., Yang, Z., Cohen, W.B., Pierce, D.J., 2006. Application of two regression-based methods to estimate the effects of partial harvest on forest structure using Landsat data. Remote Sens. Environ. 101, 115–126.
Hermosilla, T., et al., 2015. Regional detection, characterization, and attribution of annual forest change from 1984 to 2012 using Landsat-derived time-series metrics. Remote Sens. Environ. 170, 121–132.
Hirschmugl, M., Steinegger, M., Gallaun, H., Schardt, M., 2014. Mapping forest degradation due to selective logging by means of time series analysis: case studies in Central Africa. Remote Sens. 6, 756–775.
Husak, G.J., et al., 2008. Crop area estimation using high and medium resolution satellite imagery in areas with complex topography. J. Geophys. Res. 113 (D14112), 1–8.
Hussain, M., et al., 2013. Change detection from remotely sensed images: from pixel-based to object-based approaches. Isprs J. Photogramm. Remote. Sens. 80, 91–106.
Häme, T., Heiler, I., Miguel-Ayanz, J.S., 1998. An unsupervised change detection and recognition system for forestry. Int. J. Remote Sens. 19, 1079–1099.
Häme, T., et al., 2013. Improved mapping of tropical forests with optical and SAR imagery, part I: forest cover and accuracy assessment using multi-resolution data. IEEE J. Sel. Top. Appl. Earth Obs. Remote Sens. 6, 74–91.
Kangas, A., et al., 2015. Decision Support for Forest Management. Springer, Cham.
Karlsson, K.-G., 2003. A 10 year cloud climatology over Scandinavia derived from NOAA advanced very high resolution radiometer imagery. Int. J. Climatol. 23, 1023–1044.
Kennedy, R.E., et al., 2009. Remote sensing change detection tools for natural resource managers: understanding concepts and tradeoffs in the design of landscape monitoring projects. Remote Sens. Environ. 113, 1382–1396.
Kennedy, R.E., Yang, Z., Cohen, W.B., 2010. Detecting trends in forest disturbance and recovery using yearly Landsat time series: 1. LandTrendr — temporal segmentation algorithms. Remote Sens. Environ. 114, 2897–2910.
Kuuluvainen, T., 2009. Forest management and biodiversity conservation based on natural ecosystem dynamics in Northern Europe: the complexity challenge. AMBIO - J. Hum. Environ. 38, 309–315.
Kuuluvainen, T., Aakala, T., 2011. Natural forest dynamics in boreal fennoscandia: a review and classification. Silva Fenn. 45, 823–841.
Larsson, S., Danell, K., 2001. Science and the management of boreal forest biodiversity. Scand. J. For. Res. 16, 5–9.
Liasis, G., Stavrou, S., 2016. Satellite images analysis for shadow detection and building height estimation. Isprs J. Photogramm. Remote. Sens. 119, 437–450.
Luke, 2018. Silvicultural and Forest Improvement Work 2017. [Online] Available at: https://stat.luke.fi/en/silvicultural-and-forest-improvement-work [Accessed 17 6 2019]. .
Lunetta, R.S., et al., 1991. Remote sensing and geographic information system data integration: error sources and research issues. Photogramm. Eng. Remote Sensing 57, 677–687.
Matricardi, E.A., et al., 2010. Assessment of tropical forest degradation by selective logging and fire using Landsat imagery. Remote Sens. Environ. 114, 1117–1129.
Matton, N., et al., 2015. An automated method for annual cropland mapping along the season for various globally-distributed agrosystems using high spatial and temporal resolution time series. Remote Sens. (Basel) 7, 13208–13232.
Minnis, P., Liou, K.-N., Takano, Y., 1993. Inference of cirrus cloud properties using satellite-observed visible and infrared radiances. Part I: parameterization of radiance fields. J. Atmos. Sci. 50, 1279–1304.
Næsset, E., 2014. Area-based inventory in Norway – from innovation to an operational reality. In: Maltamo, M., Næsset, E., Vauhkonen, J. (Eds.), Forestry Applications of Airborne Laser Scanning. Springer, Dordrecth, pp. 215–240.
Olofsson, P., et al., 2014. Good practices for estimating area and assessing accuracy of land change. Remote Sens. Environ. 148, 42–57.
Peltoniemi, M., et al., 2018. Networked web-cameras monitor congruent seasonal development of birches with phenological field observations. Agric. For. Meteorol. 249, 335–347.
Petitjean, F., Kurtz, C., Passat, N., Cançarski, P., 2012. Spatio-temporal reasoning for the classification of satellite image time series. Pattern Recognit. Lett. 33, 1805–1815.
Pickell, P.D., et al., 2014. Monitoring anthropogenic disturbance trends in an industrialized boreal forest with Landsat time series. Remote. Sens. Lett. 5, 783–792.
Poikolainen, J., Tolvanen, A., Karhu, J., Kubin, E., 2016. Seventeen-year trends in spring and autumn phenophases of Betula pubescens in a boreal environment. Int. J. Biometeorol. 60, 1227–1236.
Pontius, R.G., Millones, M., 2011. Death to Kappa: birth of quantity disagreement and allocation disagreement for accuracy assessment. Int. J. Remote Sens. 32, 4407–4429.
Potapov, P., Turubanova, S., Hansen, M.C., 2011. Regional-scale boreal forest cover and change mapping using Landsat data composites for European Russia. Remote Sens. Environ. 115, 548–561.
Pudas, E., et al., 2008a. Trends in phenology of Betula pubescens across the boreal zone in Finland. Int. J. Biometeorol. 52, 251–259.
Pudas, E., et al., 2008b. Timing of plant phenophases in Finnish Lapland in 1997-2006. Boreal Environ. Res. 13, 31–43.
Rautiainen, M., Heiskanen, J., Korhonen, L., 2012. Seasonal changes in canopy leaf area index and MODIS vegetation products for a boreal forest site in central Finland. Boreal Environ. Res. 17, 72–84.
Richter, P., Müller, A., 2005. De-shadowing of satellite/airborne imagery. International Joural of Remote Sensing 26, 3137–3148.
Rullan-Silva, C.D., Olthoff, A.E., Delgado de la Mata, J.A., Pajares-Alonso, J.A., 2013. Remote monitoring of forest insect defoliation. A review. For. Syst. 22, 377–391.
Saarinen, N., et al., 2018. Landsat archive holdings for Finland: opportunities for forest monitoring. Silva Fenn. 52.
Sawyer, G., Dubost, A., de Vries, M., 2016. Copernicus Sentinels’ Products Economic Value: A Case Study of Forest Management in Sweden. s.l. European Association of Remote Sensing Companies.
Schroeder, T.A., Wulder, M.A., Healey, S.P., Moisen, G.G., 2011. Mapping wildfire and clearcut harvest disturbances in boreal forests with Landsat time series data. Remote Sens. Environ. 115, 1421–1433.
Senf, C., Seidl, R., Hostert, P., 2017. Remote sensing of forest insect disturbances: current state and future directions. Int. J. Appl. Earth Obs. Geoinf. 60, 49–60.
Shao, G., Wu, J., 2008. On the accuracy of landscape pattern analysis using remote sensing data. Landsc. Ecol. 23, 505–511.
Tewkesbury, A.P., et al., 2015. A critical synthesis of remotely sensed optical image change detection techniques. Remote Sens. Environ. 160, 1–14.
Verbersselt, J., Hyndman, R., Newnham, G., Culvenor, D., 2010. Detecting trend and seasonal changes in satellite image time series. Remote Sens. Environ. 114, 106–115.
Verbesselt, J., Hyndman, R., Newnham, G., Culvenor, D., 2010. Detecting trend and seasonal changes in satellite image time series. Remote Sens. Environ. 114, 106–115.
Verbesselt, J., Zeileis, A., Herold, M., 2012. Near real-time disturbance detection using satellite image time series. Remote Sens. Environ. 123, 98–108.
White, J.C., et al., 2016. Remote sensing technologies for enhancing forest inventories: a review. Can. J. Remote. Sens. 42, 619–641.
Xie, Y., Sha, Z., Yu, M., 2008. Remote sensing imagery in vegetation mapping: a review. J. Plant Ecol. 1, 9–23.
Zhu, Z., Woodcock, C.E., 2014. Continuous change detection and classification of land cover using all available Landsat data. Remote Sens. Environ. 144, 152–171.